17th World Conference on Earthquake Engineering, 17WCEE
Sendai, Japan - September 13th to 18th 2020

Full Scale Quasi-Static Testing of a New Self-Centering Damage-Avoidant Timber Brace

M. Yousef-beik[1], S. Veismoradi[2], P. Zarnani[3], A. Hashemi[4], P. Quenneville[5]

(1) *PhD Student, Auckland University of Technology, mohamad.yousefbeik@aut.ac.nz*
(2) *PhD Student, Auckland University of Technology, sajad.veismoradi@aut.ac.nz*
(3) *Lecturer, Auckland University of Technology, pouyan.zarnani@aut.ac.nz*
(4) *Post-doctoral reseach fellow, University of Auckland, a.hashemi@auckland.ac.nz*
(5) *Professor, University of Auckland, p.quenneville@auckland.ac.nz*

Abstract

Usage of timber as a structural member in multi-story structures is acquiring more demand owing to advantages that this material can offer such as aesthetic considerations, lower environmental footprint, the speed of fabrication and high strength to weight ratio, crucial in seismic prone areas. One of the efficient lateral load resisting systems (LLRSs) in timber structures is the conventional Concentrically Timber Braces (CTBs) which can deliver the required elastic stiffness for the structure in case of low to moderate seismic events. However, there is a major concern associated with their inelastic hysteretic response in terms of ductility and energy dissipation capacity essential to resist against severe earthquakes. This lack of performance is induced by the stiffness and strength degradation of timber connections under cyclic loading, known as slackness or pinching. To address these shortcomings, new Resilient Slip Friction Joints (RSFJs) are incorporated in the timber brace, thereby forming a damage-free system providing self-centring and damping with no post-event maintenance. In addition, a new anti-buckling mechanism is introduced for this system to control the stability of the brace under compression forces. The performance of this new bracing system is experimentally verified through a full-scale quasi-static test, well aligned with the predictions of the analytical model developed. Given the validation and demonstrated advantages, this new bracing system has been recently adopted in a real-life project and is expected to provide more opportunities for construction of multi-storey timber structures in active-seismic regions.

Keywords: Damage-avoidant Design, Low-damage Construction, Friction damping, Self-centering brace, Timber, RSFJ

1. Introduction

Comparable to conventional bracing systems, lateral instability of the brace can be a obstacle on the way of achieving a desired performance for the brace especially when it is subjected to compression. The root cause of this instability lies in the secondary order effect reducing the rotational stiffness of the brace. In this situation, if an rotational flexibility appears within the brace, the possibility of the buckling even increases more. Such incidence has been reported for Buckling-Restrained Braces where the flexible necking zone or the flexible end gusset plates were the main cause of the buckling [1, 2]. More specifically, while it is true that the BRB is designed to yield in compression, if the gusset plates or neck does not have the adequate strength and stiffness, a premature failure can occur sooner than the core yielding [2-5]. So as to remedy the problem, Takeuchi et al. [2, 4] employed energy methods to suggest some stability criteria with respect to the boundary conditions and the geometry of the BRB. In this regard, two stability limits have been advised, one for stiffness and one for strength, in order to confirm the perfect behaviour for BRB. Apart from that, a comparable stability criterion has been put forth by Zaboli and Clifton [5] based on the formation of a plastic mechanism.

Likewise, the origin of the instability in the proposed brace stems from the arrival of a rotational flexibility where the RSFJ is positioned. This has been shown experimentally in the past studies [6-8]. In order to tackle the buckling issue, the brace needs to be strengthened where RSFJ is located. For this

purpose, a telescopic mechanism comprising of two circular steel sections is proposed. This mechanism which will be referred to as "Anti-buckling Tubes" should have a minimum strength and stiffness so that the buckling of the strengthened system is higher than the force demand. The minimum stiffness and strength can be calculated according to the stability model that is proposed in [6, 9]. Finally, the efficiency of the ABTs is validated using a full-scale quasi-static test.

2. Quantification and solution for the instability

2.1 Quantification of Buckling Load

Similar to any compressive member, one of the main phenomena that may adversely affect the performance of a tension-compression brace is the buckling, which is normally known by premature fail due to increasing deflection to the side. The origin of the instability in the proposed brace stems from the arrival of a rotational flexibility [6, 7] where the RSFJ is positioned. In this regard, it has been shown that the RSFJ has bilinear elastic behaviour without any damping in the out-of-plane direction (Fig.1.b), while it has multi-linear flag-shape behaviour in the in-plane direction (Fig.1.c). The deformed shape of the RSFJ in in-plane and out-of-plane direction is depicted in Fig.1.d for further illustration. The following formulation has suggested and experimentally validated [6, 7, 9] to quantify the buckling load for RSFJ-brace assembly with one damper within the brace:

$$P_{cr,loading} = \frac{L\frac{d}{d\theta}\int_0^{\theta\le\theta_{ult}} M(\theta)}{L_1 L_2} \tag{1}$$

Where "L", "L1" and "L2" are defined in Fig.1.a. If tangent stiffness of rotational spring is assumed to be "$K_{tan} = \frac{d}{d\theta}\int_0^{\theta<\theta_{ult}} M(\theta)$", the critical load can be calculated as:

$$P_{cr,loading} = \frac{K_{tan} L}{L_1 L_2} \tag{2}$$

Eq.(2) indicates that the instability load of the brace is a function of the tangent stiffness of the rotational spring. It is worth mentioning that the term "tangent" refers to the phase in which damper is acting. If damper is at before-slip phase, tangent rotational stiffness shall be regarded as initial rotational stiffness (Fig.1(b, c)); however, if damper is activated, the tangent rotational stiffness shall be regarded as the post-slip (secondary) rotational stiffness. Accordingly, for a system with bilinear rotational flexibility without damping (Fig. 1.b), there are two buckling loads namely before and after-slip associated with initial and post-slip phases while for a system with bilinear rotational flexibility with passive damping (Fig. 1.c), there are three instability loads associated with before, after-slip (loading and unloading), respectively. The only parameters that are required for stability analysis of the brace are the in-plane and out-plane rotational stiffness of RSFJ to be input as the nonlinear spring in the mathematical model (Fig.1.b). Then based on Eq.(3), the associated buckling loads can be calculated. According to experimental observation, initial (before-slip) rotational stiffness is much higher than that of post-slip. Hence, the buckling with initial rotational stiffness during the before-slip phase is unlikely and not studied in this program. Eq.(3) and Eq.(4) show the post-slip stiffness of RSFJ in in-plane direction for loading and unloading phase while Eq.(5) shows the post-slip rotational stiffness of RSFJ in the out-of-plane direction (shown in Fig.1.c, d)). If these stiffnesses are replaced in Eq.(2), the associated buckling loads can be carried out.

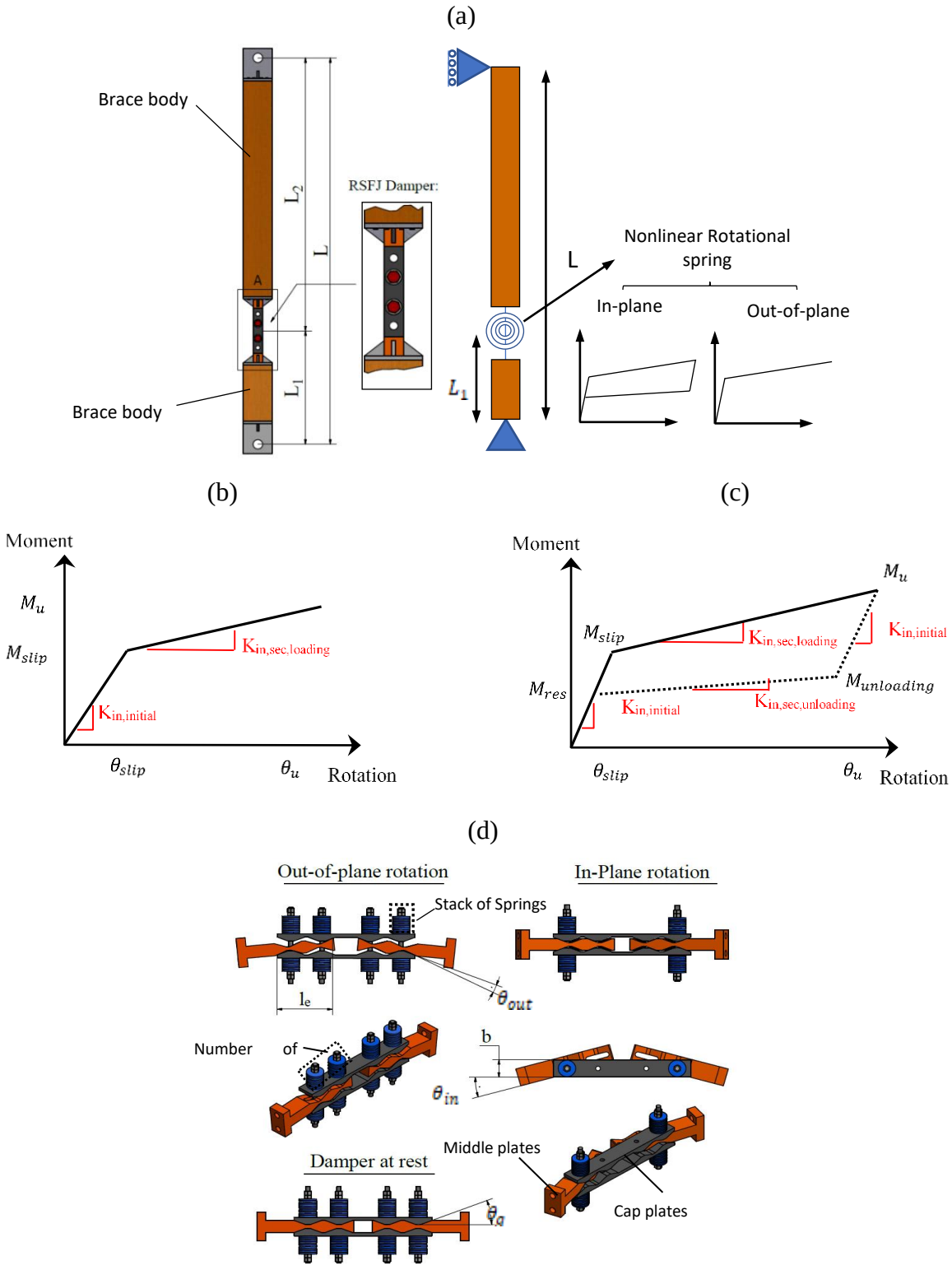

Fig. 1 – (a) intended brace configuration, (b) bilinear rotational spring without damping (out-of-plane rotational behaviour of RSFJ), (c) flag-shape rotational spring (in-plane rotational behaviour of RSFJ), (d) deformed shape of RSFJ in in-plane and out-of-plane

$$K_{in,sec,loading} = \frac{n_b K_{st} b^2}{2}\left(\frac{2sin^2\theta_g + \mu sin2\theta_g}{2sin^2\theta_g - \mu sin2\theta_g}\right) \tag{3}$$

$$K_{in,sec,unloading} = \frac{n_b K_{st} b^2}{2}\left(\frac{2sin^2\theta_g - \mu sin2\theta_g}{2sin^2\theta_g + \mu sin2\theta_g}\right) \tag{4}$$

$$K_{out,sec} = \frac{n_b K_{st} L_e^2}{4} \tag{5}$$

In Eq.(3)- Eq.(5), "b" is width of cap plates, "K_{st}" is the stiffness of disc spring stack and "L_e" is overlap length between cap and middle plate. The assemblage of a RSFJ damper at different poses is depicted in Fig.3. As it can be observed, all of the post-slip rotational stiffnesses are directly dependent on stiffness of a stack and number of bolts. Moreover, the in-plane post-slip stiffness is directly correlated with width of cap plates while out-of-plane post-slip stiffness depends on overlap length between cap and middle plate.

2.2 Solution to buckling

In case that the calculated buckling load of the brace is less than the force demand in the brace, the buckling occurrence is almost curtain, which indeed results in performance interruption once the brace is loaded in compression. As it was discussed earlier, the flexibility that arrives with installation of the damper is the main reason due to which RSFJ-brace assembly can buckle. A reasonable way to tackle the issue is the local strengthening of where RSFJ is located. The whole process of the strengthening should be based on fact that the new buckling of the strengthened system should be higher than the force demand. This process is schematically depicted in the flowchart shown in Fig.3. For the purpose of local strengthening, a telescopic configuration comprising of two sliding circular tubes is used whereby the rotational stiffness of the brace at the location of the RSFJ is increased (shown in Fig.2). The important point that should be taken into consideration is that these two sliding tubes should possess the required stiffness and strength so that the global buckling load of the strengthened system be higher than the force demand in the brace. In order to quantify this, the same model explained in previous section can be used based on the premise that the Anti-buckling Tubes (ABT) and damper(s) act in parallel. Therefore, the input rotational stiffness into stability model should be assumed to be the summation of the dampers' rotational stiffness and ABTs' rotational stiffness. The strengthened rotational stiffness can be approximated based on the well-known virtual work method and is formulated in Eq. (6):

$$\left(K_{tan}\right)_{strengthened} = \left(K_{tan}\right)_{RSFJ} + 3\left(\frac{EI}{L}\right)_{ABT} \times m \tag{6}$$

$$m = \frac{\xi_2}{\left[\beta_b\left(1-\xi_2\right)^3 + \left(\xi_2-\xi_1\right)^3 - 3\left(\xi_2{}^2 - \xi_1{}^2\right) + 3\left(\xi_2 - \xi_1\right)\right]} \tag{7}$$

$$\beta_b = \frac{EI_{ABT}}{EI_{brace}} \tag{8}$$

$$\xi_1 = \frac{L_1}{L},\ \xi_2 = \frac{L_1 + 0.5L_{RSFJ}}{L} \tag{9}$$

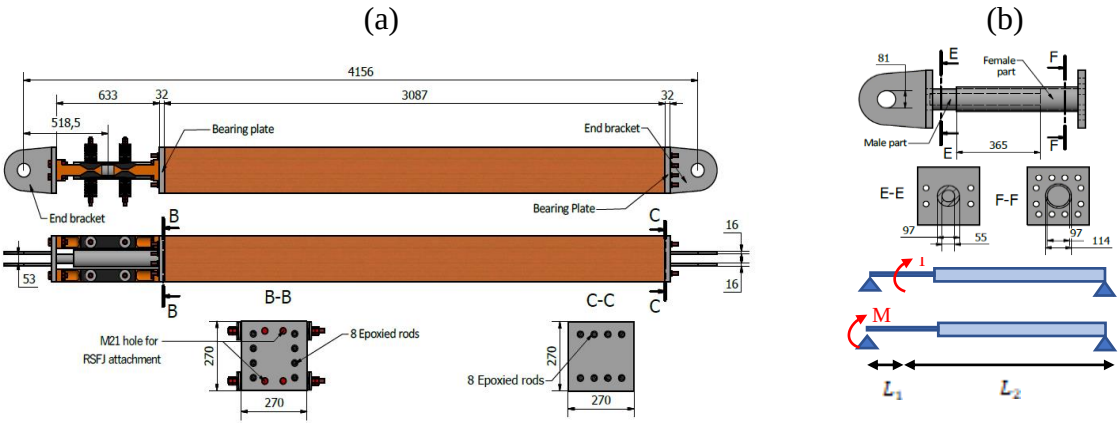

Fig. 2 – (a) drawing for the timber brace with ABTs, (b) drawing for Anti-buckling tubes for ABM,

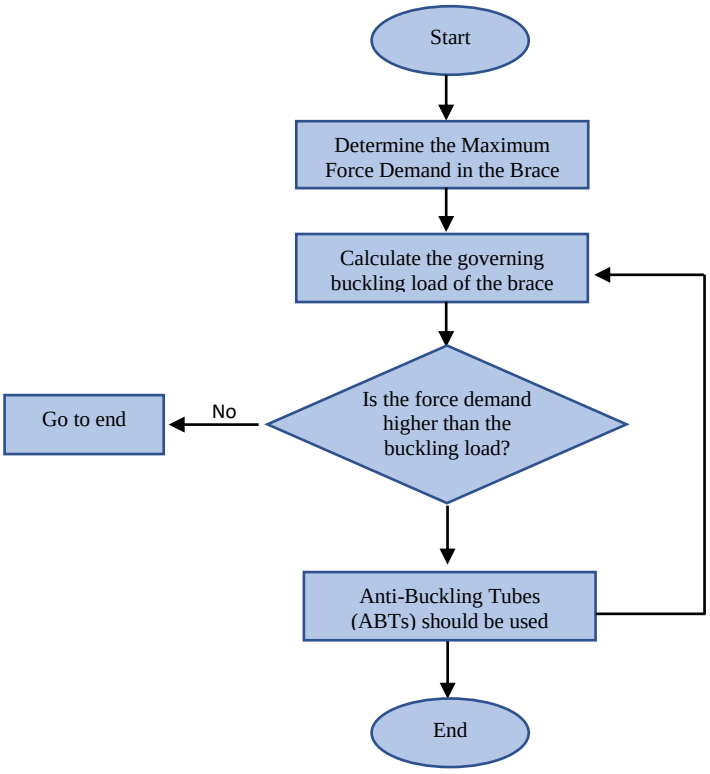

Fig. 3 – Design Flowchart of RSFJ-brace assembly

3. Experimental Validation

3.1 Test Setup

The test setup for full-scale quasi-static test is shown in Fig.4. The vertical steel column was composed of the PFC sections that were welded using batten plates. This column was supposed to transfer the axial tension force of the brace to the strong floor. They were also two lateral supports erected besides the

specimen with the intension of limiting the out-of-plane displacement of the specimen and stabilizing the actuator movement. The whole setup and the steel connections were designed elastically in a way that the brace force can reach up to 400 kN force. The 250 kN MTS actuator with a stroke capacity of ±125 mm were positioned at the height of 4250 mm from the strong floor to execute the loading protocol. For data acquisition, one LVDT and one drew wire were utilized to measure the joint and brace response, respectively during the test. The test setup and instrumentation system is depicted in Fig.4. The RSFJ-brace specimen was borrowed from a real under-construction project in New Zealand which was employed in a chevron configuration within a frame with 3340 m height and 6750 m width. The brace body was composed of a timber Glue-Lam GL8 grade with an elastic modulus of 8 GPa. The cross-section of the specimen was square-shaped with 270 mm width. Two RSFJs with 200 kN capacity (shown in Fig.4.e) were attached to the end of the brace to provide the energy-dissipation and self-centering characteristic. The target force and displacement for the brace specimen were 400 kN at 50mm, respectively. The instability load of the brace without using the anti-buckling tubes was extremely low (20 kN). Therefore, the procedure explained in flowchart in Fig.3 were employed to design a proper anti-buckling tube. In this respect, the two sliding CHS sections depicted in Fig.2.b were utilized from the available CHS sections. The new buckling load of the strengthened system was around 1343 kN.

(a)

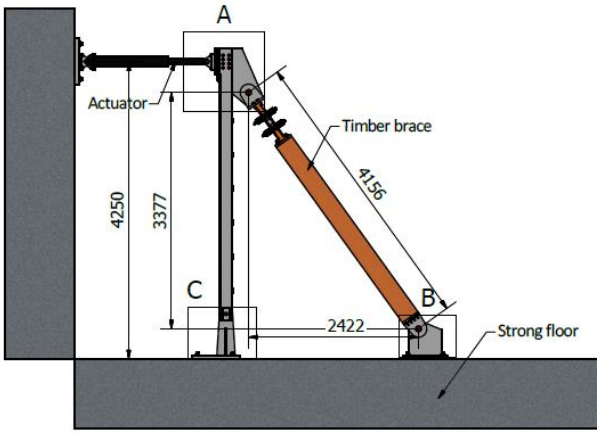

(b)

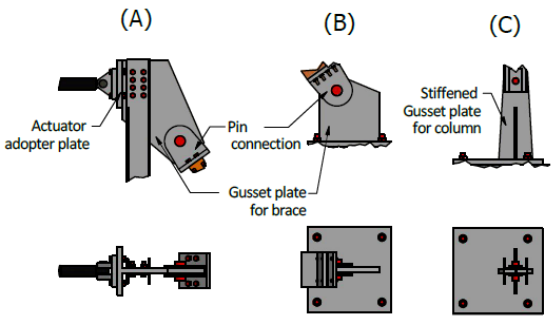

(c)

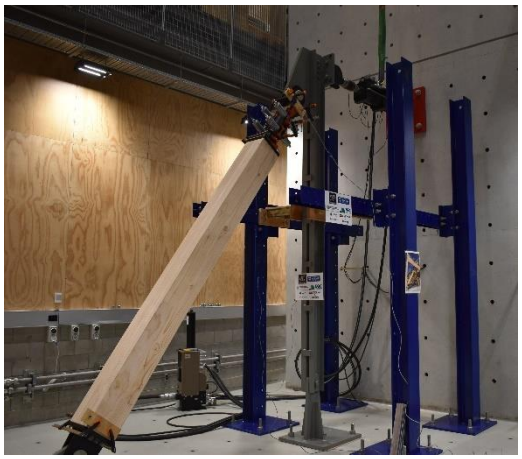

(d)

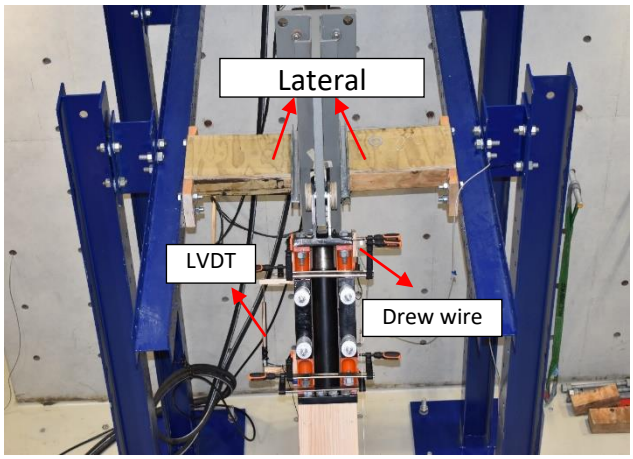

(e)

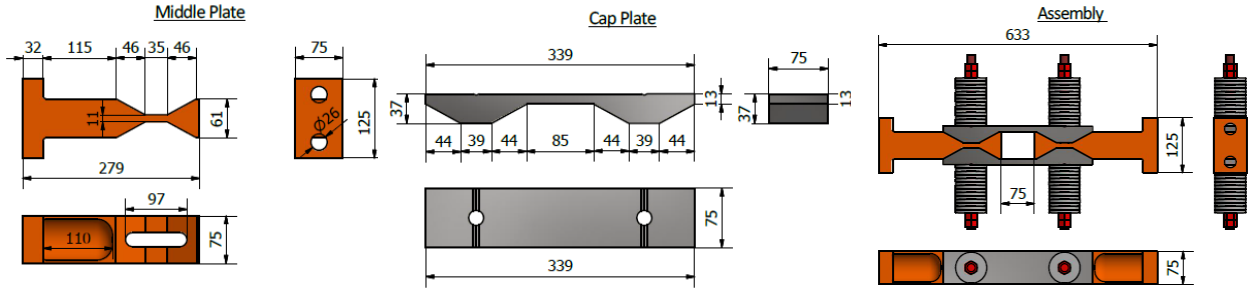

Fig. 4 – (a) side view, (b) top view, (c) front view and (d) setup in reality, (e) Utilized RSFJ with 200 kN capacity

3.2 Full-scale test results

The RSFJ-brace specimen was tested using the following reversed cyclic test to further investigate the brace behaviour. More specifically, the main aim of the study was to validate the ABTs performance in terms of postponing the buckling incidence. The load protocol was designed according AISC 341 standard suggestion which is originally for Buckling-Restrained Braces. The reason for this lies in the fact that there is no specially designed load protocol for self-centring braces. However, due to strict requirements of the BRB load protocol suggested by AISC 341, it is used for testing the self-centring braces as well [10]. It is worth nothing that this protocol necessitates that the brace should possess twice the ductility capacity of the design story drift together with an accumulative inelastic axial ductility capacity ratio of 200. For further information, it can be referred to [11]. The loading rate used for the test was 0.3 mm per second, similar to what was used for the component testing.

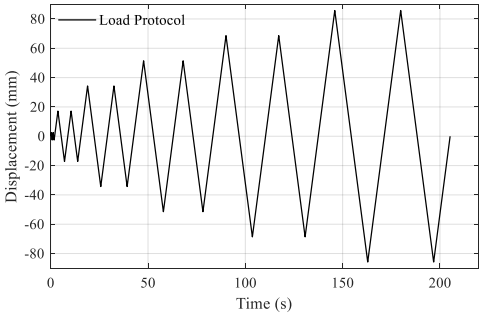

Fig. 5 – Load protocol applied to the brace via actuator

Fig.6 illustrates the performance of the RSFJ timber brace subjected to mentioned loading regime. Fig.6.a shows the brace force and the drew wire readings including the internal deflection of timber, timber connection and the RSFJs. Fig.6.b shows the brace force and the LVDT's reading which is limited to RSFJ displacement. As can be vividly observed, no instability or sign of buckling in the compression was witnessed and the flag-shaped seemed completely symmetrical. This demonstrates the effectiveness of the ABT.

(a) (b)

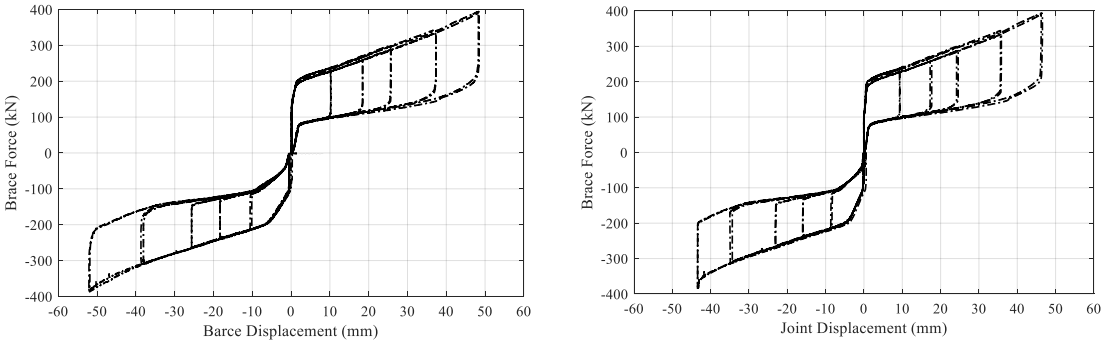

Fig. 6 – Brace Performance (a) Brace force VS Brace displacement, (b) Brace force VS RSFJ displacement

4. SUMMARY AND CONCLUSION

A new Self-centring timber brace is introduced that utilizes the RSFJ dampers for energy dissipation. According to past studies, the instability and buckling in loading and unloading was observed for the brace which resulted in capacity reduction of the brace in compression though they were of elastic type and did not bring any damage. The root cause of the problem was observed to be the flexibility that appears as a result of damper installation. A telescopic mechanism comprising of two circular sliding steel sections was suggested as the local strengthening to postpone the buckling load to a value higher than the force demand. A full-scale quasi-static test was performed to evaluate the effectiveness of the proposed solution. According the experimental observations, no buckling was witnessed in the compression zone, the complete symmetrical flag-shape performance was achieved for the RSFJ-brace specimen.

5. ACKNOWLEDGEMENT

The authors would like to thank the Earthquake Commission (EQC) of New Zealand and the Ministry of Business, Innovation and Employment of New Zealand (MBIE) for the financial support provided for this research. Also, the contribution of technicians Allan Dixon, Mark Byrami, Andrew Virtue and Dave Croft, and the intern student Renan Louvel in the preparation of both test setups in both Auckland University of Technology Built environment Lab and The University of Auckland Structural test Hall are appreciated. The commercial interest for Tectonus company providing the RSFJ specimens is appreciated.

6. References

[1] Lin, P.C., et al., Seismic design and hybrid tests of a full-scale three-story buckling-restrained braced frame using welded end connections and thin profile. Earthquake Engineering & Structural Dynamics, 2012. 41(5): p. 1001-1020.

[2] Takeuchi, T., et al., Out-of-plane stability of buckling-restrained braces including moment transfer capacity. Earthquake Engineering & Structural Dynamics, 2014. 43(6): p. 851-869.

[3] Hikino, T., et al., Out-of-plane stability of buckling-restrained braces placed in chevron arrangement. Journal of Structural Engineering, 2012. 139(11): p. 1812-1822.

[4] Takeuchi, T., R. Matsui, and S. Mihara, Out-of-plane stability assessment of buckling-restrained braces including connections with chevron configuration. Earthquake Engineering & Structural Dynamics, 2016. 45(12): p. 1895-1917.

[5] Zaboli, B., G. Clifton, and K. Cowie, Out-of-plane stability of gusset plates using a simplified notional load yield line method. 2017.

[6] Yousef-beik, S.M.M., et al., New Seismic Damage Avoidant Timber Brace Using Innovative Resilient Slip Friction Joints For Multi-story Applicatios, in Word Conferrence on Timber Engineering (WCTE). 2018: Seoul, Korea.

[7] Hashemi, A., et al., Seismic performance of a damage avoidance self-centring brace with collapse prevention mechanism. Journal of Constructional Steel Research, 2019. 155: p. 273-285.

[8] Zarnani, P., et al., ROTATIONAL PERFORMANCE OF RESILIENT SLIP FRICTION JOINT (RSFJ) AS A NEW DAMAGE FREE SEISMIC CONNECTION.

[9] Yousef-beik, S.M.M., et al., Lateral Instability of Self-centring Braces: Buckling in loading and Unloading, in Pacific Conference on Earthquake Engineering. 2019: Auckland, New Zealand.

[10] Erochko, J., C. Christopoulos, and R. Tremblay, Design, testing, and detailed component modeling of a high-capacity self-centering energy-dissipative brace. Journal of Structural Engineering, 2014. 141(8): p. 04014193.

[11] AISC:341, AISC 341-10, Seismic Provisions for Structural Steel Buildings. Chicago, IL: American Institute of Steel Construction, 2010.

